Solar Energy Vol. 33, No. 3/4, pp. 343–351, 1984
Printed in the U.S.A.

0038-092X/84 $3.00 + .00

SOLAR IRRADIANCE ON FLAT-PLATE COLLECTORS IN URBAN ENVIRONMENTS

C. M. Rowe and C. J. Willmott
Center for Climatic Research, Department of Geography, University of Delaware, Newark, DE 19716, U.S.A.

(*Received* 29 *July* 1983; *accepted* 11 *June* 1984)

Abstract—A numerical climatic model has been developed in order to simulate the solar irradiance that would be available to a flat-plate collector sited at street level within a typical urban setting. Results confirm that the available irradiance can be substantially reduced by the presence of horizonal obstructions. It is additionally evident that the optimal collector azimuth may vary by as much as 60° from due south—in the mid-latitude northern hemisphere. Losses of available irradiance, associated with the popular practice of facing collectors due south and tilting them as a simple function of latitude, appear to be as high as 10–15% when compared to the total solar irradiance available at an optimal collector orientation as determined by simulation.

1. INTRODUCTION

In addition to its climatic dependence, solar energy available to a fixed, flat-plate solar collector—or any flat surface is significantly controlled by both the orientation of the collector or other surface of interest and the structure of the surrounding environment. One consequence is that the collector orientation which would receive the greatest total irradiance over a time period of interest—the optimal orientation—frequently cannot be determined by the various simple 'rules' cited in the engineering literature.† Such rules often inappropriately face the collector due south (in the northern hemisphere), and tilt it as a simple function of the latitude of the site and the time of year when maximum energy receipt is desired. Horizonal obstructions (e.g. buildings, trees and hills) in a collector's field of view or consistent seasonal or diurnal asymmetries in global irradiance (e.g. due to morning fog or afternoon clouds), in particular, can shift the optimal orientation of a collector as much as 15° from a simple rule-determined orientation [1, 2]. In addition, horizonal obstructions can significantly decrease the total amount of irradiance on the collector [1–3]. Many previous simulations of the optimal orientation of flat-plate solar collectors—which were performed for a single azimuth [4, 5] or for daily or monthly irradiance totals [6]—also have not adequately accounted for the presence of horizonal obstructions or asymmetries in global irradiance. As a result, past agreement between simple rule- and simulation-determined optimal orientations may be somewhat spurious. By simulating the hourly fluxes of direct, diffuse and reflected radiation in a realistic environment, however, the climatically and environmentally optimal orientation of the collector can be adequately determined.

In order to further investigate total solar irradiance on flat-plate solar collectors—or any planar surface—a numerical, climatic model was assembled and hourly simulations for a hypothetical urban environment were performed. The model is described in Sections 2 and 3 of this paper, followed by a discussion of the pertinent short-wave fluxes associated with a flat-plate solar collector located in a hypothetical 'city' erected at Sterling, Virginia.

† Various rules of thumb have been suggested for the siting of fixed, flat-plate collectors depending on the time period over which the collector is to be active. These methods generally (1) assume diurnal symmetry in available solar radiation and (2) recommend a fixed azimuth of 180° in the northern hemisphere, while adjusting the tilt to maximize the theoretical, clear-sky direct-beam irradiance. If maximum annual energy receipt is desired, a tilt equal to the latitude of the site is recommended. For maximum winter energy receipt, the tilt should be increased, and for maximum summer energy receipt, the tilt should be less than the latitude in order to compensate for the change in average solar elevation. The suggested amount of this increase or decrease ranges from 10° to 20°, with ±15° commonly used [4, 5, 24, 27–30].

2. IRRADIANCE COMPUTATIONS FOR UNOBSTRUCTED SURFACES

Beginning with measured or predicted global irradiance for an unobstructed environment, the computation of collector irradiance first requires a determination of the direct and diffuse portions of global irradiance. These direct and diffuse irradiances are then modified to account for the anisotropy of sky-diffuse radiation and the collector orientation. In addition, estimates of the irradiance reflected from the ground onto the collector are made.

Liu and Jordan [7] were first to develop a simple statistical relationship between the diffuse fraction of global irradiance and a clearness index which is

defined as the proportion of extraterrestrial radiation reaching the ground. Their relationship applies strictly to daily values, although a number of researchers have re-specified and used it in hourly computations with some success. Erbs [8], for instance, developed a credible function from over 19,000 hourly values of diffuse and global irradiance which were observed at four locations in the United States. His equation is

$$\frac{H_{hd}}{H_h} = \begin{cases} 1.0 - 0.09k_T, & k_T \le 0.22 \\ 0.9511 - 0.1604k_T + 4.388k_T^2 - 16.638k_T^3 + 12.336k_T^4, & 0.22 < k_T \le 0.80 \\ 0.165, & k_T > 0.80 \end{cases} \quad (1)$$

where H_{hd} is the total sky-diffuse irradiance on a horizontal surface, H_h is global irradiance and k_T is the hourly clearness index (H_h/H_o). Evaluation of this relationship with data from Highett, Australia, and Seattle-Tacoma, Washington, suggests that it is location-independent [9]. Furthermore, because of the high quality of the data used to derive Erbs' relationship, eqn (1) is thought to be superior to other such relationships—especially when used in the conterminous United States [1]. Equation (1), therefore, is used in the present study to estimate the diffuse fraction of global irradiance. Total sky-diffuse irradiance on a horizontal surface subsequently can be determined by multiplication of the diffuse fraction (H_{hd}/H_h) by H_h. Horizontal, direct-beam irradiance (H_{hb}) then constitutes the remaining portion of global irradiance, i.e. $H_{hb} = H_h - H_{hd}$.

In order to compute solar irradiance on sloping collector surfaces, each component of global irradiance must be adjusted for the non-horizontal surface orientation. Irradiance reflected from the surrounding ground surface which is incident on the collector also must be considered. Direct-beam irradiance on any collector of orientation i (H_{ib}) is given by

$$H_{ib} = H_{nb} \cos \theta_i \quad (2)$$

where H_{nb} is normal incidence beam irradiance and θ_i is the angle between the normal to the collector surface and the sun's rays. The unknown normal irradiance is obtained from

$$H_{nb} = H_{hb}/\cos \theta_z \quad (3)$$

where θ_z is the angle of the sun from the local zenith. The anisotropic distribution of sky-diffuse radiation over the sky-dome can be accounted for by way of its dependence on cloud cover and atmospheric transmissivity [10–15]. Using anisotropy indices developed by Hay [16], for example, the proportion of anisotropic sky-diffuse irradiance on sloping (κ_i) and horizontal (κ_h) surfaces can be adequately estimated. Hay's anisotropy index for sloping surfaces is

$$\kappa_i = (H_{nb}/H_{sc}) \cos \theta_i. \quad (4)$$

Assuming that all anisotropic radiation is circumsolar, anisotropic sky-diffuse irradiance on the collector can be expressed as

$$H_{ida} = H_{hd}\kappa_i/\cos \theta_z \quad (5)$$

while isotropic sky-diffuse irradiance on the collector becomes

$$H_{idi} = H_{hd}(1 - \kappa_h/\cos \theta_z)[(1 + \cos \beta)/2] \quad (6)$$

where β is the tilt angle of the collector. Reflected solar radiation can represent a large contribution to the total irradiance on a collector, especially when the ground is covered by snow or the collector is nearly vertical. When it is assumed that the ground is a level, perfectly diffuse reflector of constant albedo (ρ), diffuse ground-reflected irradiance on the collector can be estimated by

$$H_{idr} = H_h\rho[(1 - \cos \beta)/2]. \quad (7)$$

Total irradiance on a collector in the absence of obstructions then is

$$H_i = H_{ib} + H_{idi} + H_{ida} + H_{idr}. \quad (8)$$

Each of these terms must be corrected for the effect of horizonal obstructions when considering a collector in an obstructed environment.

3. OBSTRUCTION EFFECTS

Probably the most significant effect of an obstruction on the amount of energy reaching a collector is the complete attenuation of beam radiation (i.e. shadowing), and this usually is the only influence considered when irradiance in an obstructed environment is evaluated [3, 17–19]. However, horizonal obstructions also will reduce the sky-diffuse and ground-reflected irradiances and they (the obstructions) may augment the total collector irradiance with irradiance reflected from the obstructions onto the collector. This model assumes that (1) the collector is a differential element with one edge along the ground, (2) each obstruction is rectangular and of constant albedo and (3) the ground is level and does not obstruct the collector's view of any obstruction. Oddly-shaped obstructions or obstructions with variable albedoes can be specified merely by subdividing the obstruction(s) into smaller, homogeneous rectangles which approximate the original obstruction(s). Since the model also assumes that all anisotropic sky-diffuse radiation is circumsolar, both the direct-beam and anisotropic-diffuse

irradiance terms are considered to be zero when the sun is behind an obstruction.

Obstruction effects on isotropic sky-diffuse and ground-reflected components are less easily determined. Because the collector is adjacent to the ground, each obstruction will block a portion of the sky seen by the collector, and those obstructions with an edge along the ground will additionally obstruct a portion of the ground seen by the collector. The amount of diffuse irradiance from both these sources thereby will be reduced. Willmott [1] considered a single obstruction situated on the ground and reduced both of these irradiance components by the total view factor [20] of the obstruction, although this assumption is somewhat arbitrary. For collectors adjacent to the ground, the reduction in radiation reflected from the ground, for example, is more closely related to the length of the obstruction edge along the ground than to the obstruction's view factor with the collector.

With regard to isotropic sky-diffuse irradiance, our reduction is equal to the decrease in the amount of sky viewed by the collector or, more precisely, it is a function of the tilt of the collector and the total view factor that all obstructions have with the collector. Since the view factors are expressed as a proportion of the view hemisphere and the amount of sky seen by a non-horizontal collector is less than a hemisphere, the sky-diffuse irradiation—corrected for horizonal obstruction—can be expressed as

$$H'_{idi} = H_{idi}\left[1 - \frac{\sum_j F(\Delta A_j \rightarrow dA_i)}{(1 + \cos\beta)/2}\right] \quad (9)$$

where $F(\Delta A_j \rightarrow dA_i)$ is the view factor between the jth obstruction and the collector. A similar reduction in ground-reflected diffuse irradiance must be determined for the subset of obstructions that are situated on the ground. Each of these obstructions obscures a segment of an infinitely large semicircle of ground located in front of and radiating from the collector [2]. In order to determine the magnitude of the irradiance reduction associated with the obscured portions of this semicircle a limit must be placed on the size of the area which reflects non-trivial amounts of radiation onto the collector. Reflection from areas greater than 50 m from the collector can be considered negligible; hence, a 50 m semicircle of ground which reflects radiation onto the collector can be defined. Ground-reflected irradiance on the collector, corrected for obstructions, then may be estimated by

$$H'_{idr} = H_{idr}\{1 - [(\sum G_j)/(\pi r^2/2)]\} \quad (10)$$

where G_j is the area of that portion of the semicircle with radius r (50 m) behind the jth obstruction. Shadowing of the ground between the collector and the obstructions, which would further reduce ground-reflected irradiance, is not considered in the present study.

An additional source of collector irradiance which must be considered—reflection from the obstructions—involves the computation of irradiance on each obstruction and the view factor between each obstruction and the collector. Each obstruction is divided into finite areas of approximately 1 m^2, with a maximum of 25 such elemental areas per obstruction. For obstructions larger than 25 m^2, the elements are enlarged so that there are no more than 25 elements. The view factor between each element and the collector is computed and used to determine the obstruction-reflected irradiance on the collector. Irradiance on each obstruction element is estimated using eqns (2)–(8) where each element is treated as if it were a collector surface. Beam and anisotropic sky-diffuse irradiance on each obstruction element then are corrected for shadowing by other obstructions. No correction of isotropic sky- and ground-reflected diffuse irradiance on the obstruction elements is made and multiple reflections are not considered. Total irradiance on an obstruction element subsequently can be estimated by

$$H'_{ij} = H'_{ibj} + H'_{idaj} + H_{idij} + H_{idrj} \quad (11)$$

where H'_{ibj} and H'_{idaj} are corrected beam and anisotropic sky-diffuse irradiances, respectively, and H_{idij} and H_{idrj} are the uncorrected isotropic sky- and ground-reflected diffuse irradiances, respectively, on the obstruction element. It follows that the total irradiance on the collector due to reflection from obstructions can be found by

$$H_{idro} = \sum_j H'_{ij}\rho_j F(\Delta A_j \rightarrow dA_i) \quad (12)$$

where ρ_j is the albedo of the jth obstruction. Finally, total irradiance on a collector with an obstructed horizon can be expressed as the sum of the corrected irradiance components

$$H'_i = H'_{ib} + H'_{ida} + H'_{idi} + H'_{idr} + H_{idro}. \quad (13)$$

4. SIMULATION RESULTS

Climatic inputs to the model are hourly totals of extraterrestrial and global irradiance as well as a snow cover indicator which is used to adjust the ground albedo for snow accumulation. These independent variables were obtained from the typical meterological year (TMY) data set [21] for Sterling, Virginia—one of 26 locations where observed global irradiances are available—and were used to evaluate the effect of horizonal obstructions on (1) the amount of radiation received by and (2) the optimal orientation of a fixed, flat-plate solar collector. Owing to computer limitations, simulations were restricted to one week per run although they

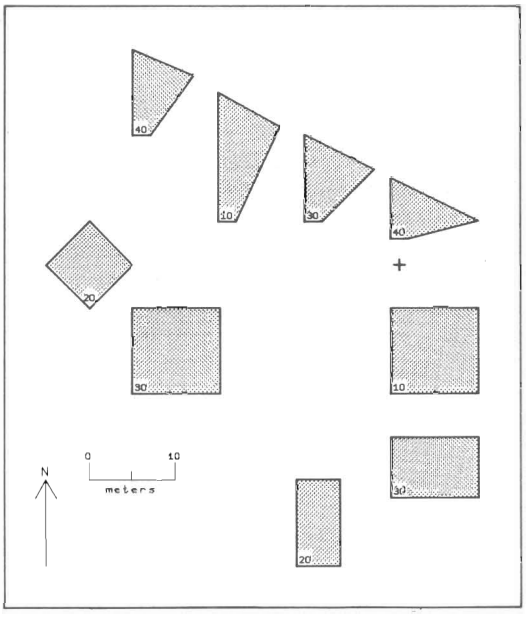

Fig. 1. Plan of the hypothetical city used in all obstructed simulations [2, 22]. The collector location is indicated by the cross while the number in the lower corner of each building is its height (m).

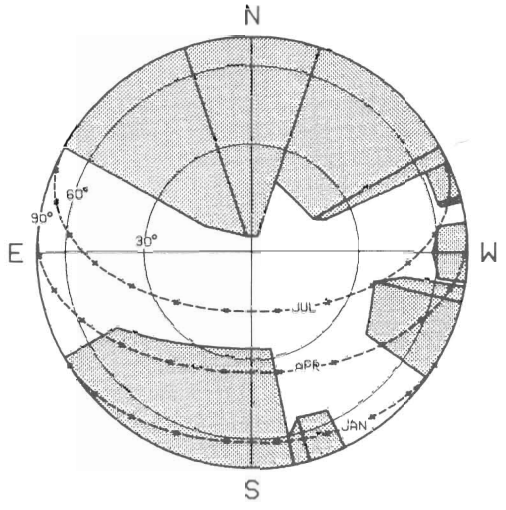

Fig. 2. Urban sky dome as viewed by a horizontal collector located at the site indicated in Fig. 1 [2]. The shaded area represents the portion of the collector's sky dome obstructed by buildings. The path of the sun and its position at the midpoint of each hour (x) for the third day of each simulated week is also plotted. It should be noted that the view is opposite planimetric, resulting in an apparent reversal of east and west.

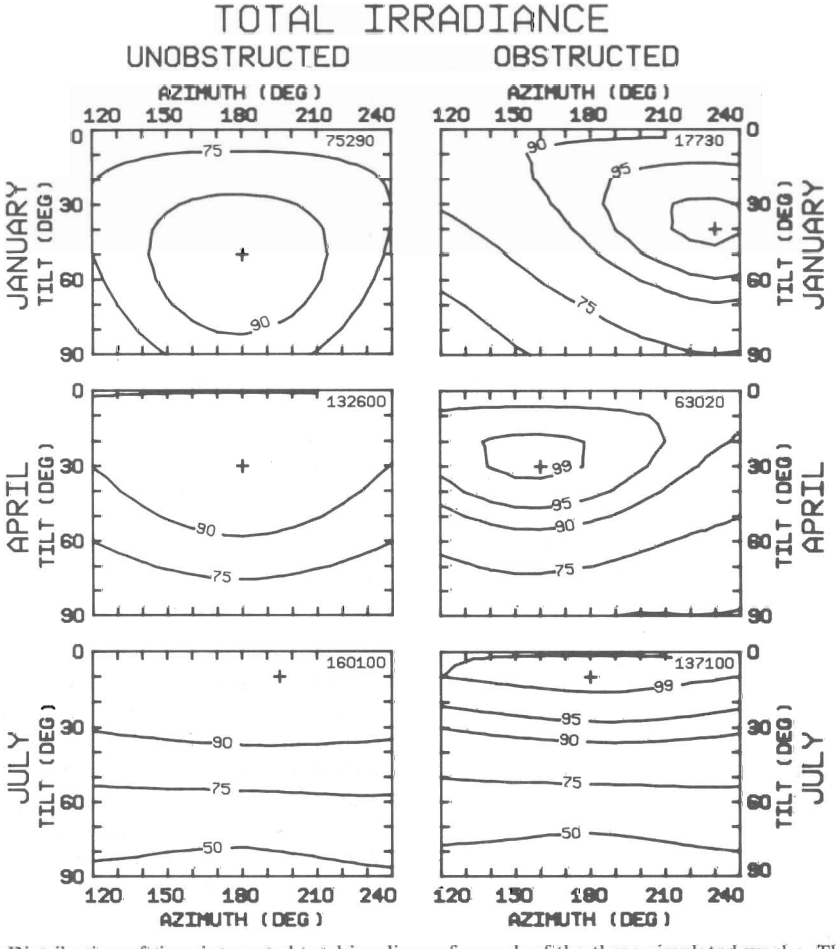

Fig. 3. Distribution of time-integrated total irradiance for each of the three simulated weeks. The '+' marks the collector orientation of maximal total irradiance receipt (given in the upper right-hand corner of each map (kJ m^{-2})) and the isolines are percentages of that maximum.

should be representative of longer periods. In order to investigate seasonal variation, the first week of January, April and July were simulated since they exemplify winter (low-sun), spring (middle-sun) and summer (high-sun) solar geometries.

A hypothetical urban environment, adapted from the 'arbitrary block model' of Frank *et al.* [22], was used in the obstructed horizon simulations. Over half the blocks were removed, however, and the remainder were shortened by half in order to achieve a more typical urban configuration (Fig. 1). Simulations were made for each of the three weeks at three locations within this 'city' as well as for a control environment (i.e. with an unobstructed horizon). Only the results from the unobstructed case and a single urban site are presented here, however—additional results are given by Rowe [2]. A fisheye view of the sky dome from the collector site provides a visual impression of the degree to which the horizon is obstructed, and it also shows the sun-path for the middle of each week (Fig. 2).

Input data necessary to define the collector environment are the x-, y- and z-coordinates of the four corners of each rectangular obstruction face, as measured from the collector position, and the albedo of each obstruction and the ground. All obstructions were assigned an albedo of 0.25 and the ground was assumed to have an albedo of 0.15—both values are typical of urban surfaces [23]. When snow was on the ground, its albedo was raised to 0.50 which is representative of patchy or old snow.

In order to examine the relationship between collector irradiance and orientation, short-wave irradiance on a 1 m^2 collector surface was computed for an array of tilts from 0° (horizontal) to 90° (vertical), and azimuths from 120° to 240° in 10° increments of tilt and azimuth. This resulted in 10 × 13 output matrices of total irradiance and each of its components. For each simulated week, isoline maps of the distribution of time-integrated total, beam, sky-diffuse and reflected irradiance in tilt–azimuth space were drawn and are presented (Figs. 3–6).

In the absence of obstructions, the patterns of total irradiance (Fig. 3) are quite similar to those reported by Willmott [1] for seasonal totals. This suggests that the weekly-derived distributions are representative of longer time periods, such as

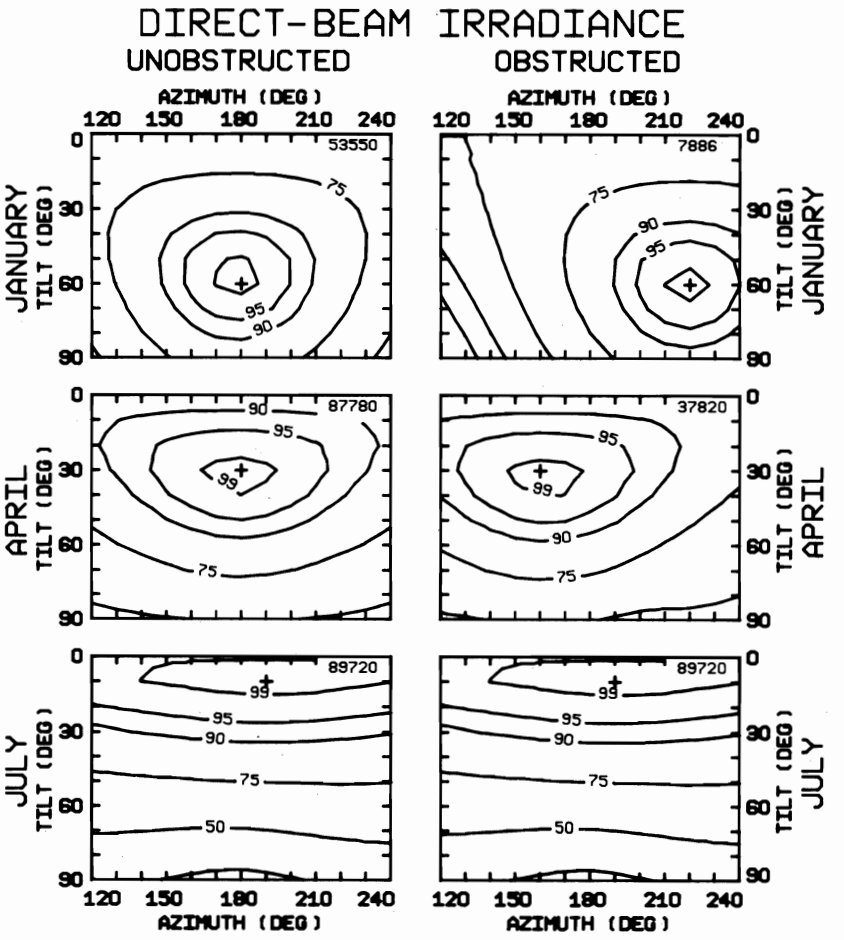

Fig. 4. Distribution of time-integrated direct beam irradiance for each of the three simulated weeks. The '+' marks the collector orientation of maximal direct beam irradiance receipt (given in the upper right-hand corner of each map (kJ m^{-2})) and the isolines are percentages of that maximum.

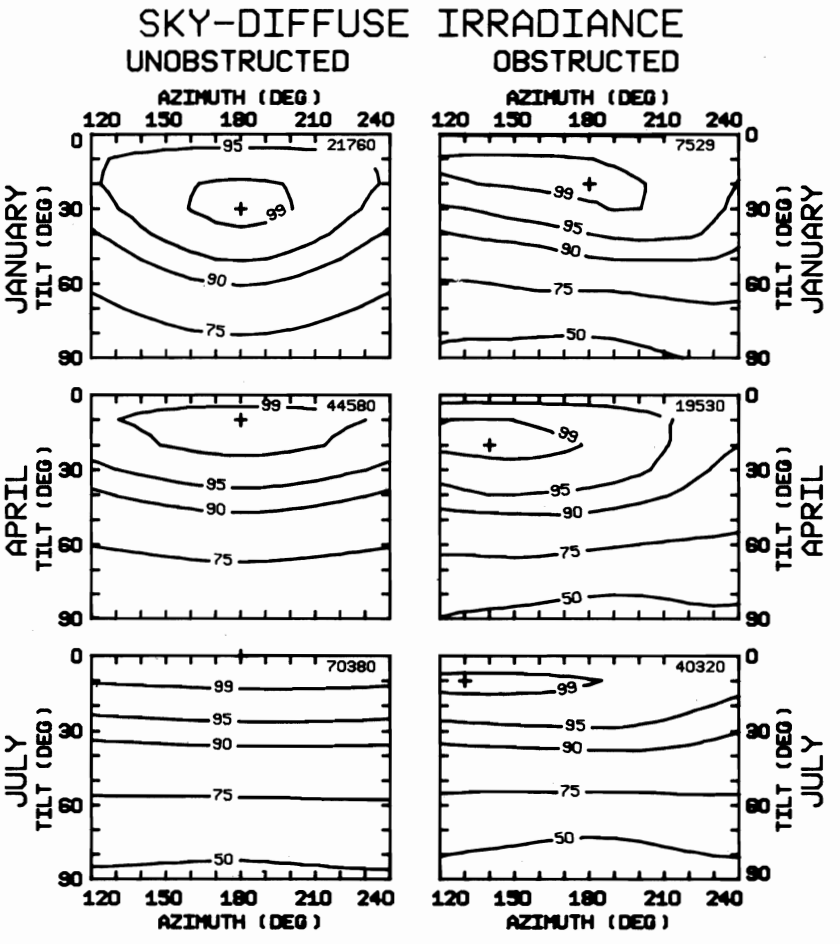

Fig. 5. Distribution of time-integrated sky-diffuse irradiance for each of the three simulated weeks. The '+' marks the collector orientation of maximal sky-diffuse irradiance receipt (given in the upper right-hand corner of each map (kJ m^{-2})) and the isolines are percentages of that maximum.

months or seasons. Climatically optimal orientations for unobstructed collectors conform quite closely to many of the rule-determined optima associated with seasonal solar energy utilization [24], while the irradiance distributions in tilt–azimuth space support the contention that orientations within 15° of the optimum will result in energy losses of less than 5%.

Direct-beam irradiance (Fig. 4) generally contributes over half of the total irradiance on collectors whose tilt and azimuth are within the range studied here. Sky-diffuse irradiance (Fig. 5) adds most of the remainder, although reflection from the ground can be significant for highly tilted collectors, especially when there is snow on the ground. Most of the sky-diffuse irradiance (55–90%) as well as all ground-reflected irradiance is assumed to be isotropic which tends to dampen the energy loss associated with climatically non-optimal azimuths. The actual distribution of ground-reflected radiation, in particular, may be highly anisotropic [11, 25]. When the horizon is substantially obstructed, the interception of isotropic sky-diffuse and ground-reflected radiation becomes azimuth dependent, due to the screening of portions of both sky and ground by the obstructions (Fig. 6).

Because direct-beam irradiance is the largest component of total irradiance on an optimally oriented collector in an unobstructed setting, shadowing of a collector by obstructions would be expected to decrease the total irradiance on the collector. This is precisely what happens in the January and April simulations, when the collector is in shadow for all but a few hours of each day. In addition, the optimal orientations for these simulations shift in order to maximize the receipt of the available direct-beam radiation (Figs. 3 and 4). It is worth noting that, in January, the optimal tilt is reduced so as to capture more isotropic sky-diffuse radiation (Fig. 5) and radiation reflected onto the collector from the large building to the north (Fig. 6).

In July, the sun is behind an obstruction only for the 2 h just prior to sunset which results in no appreciable decrease in either direct beam or anisotropic sky-diffuse irradiance. All of the reduction

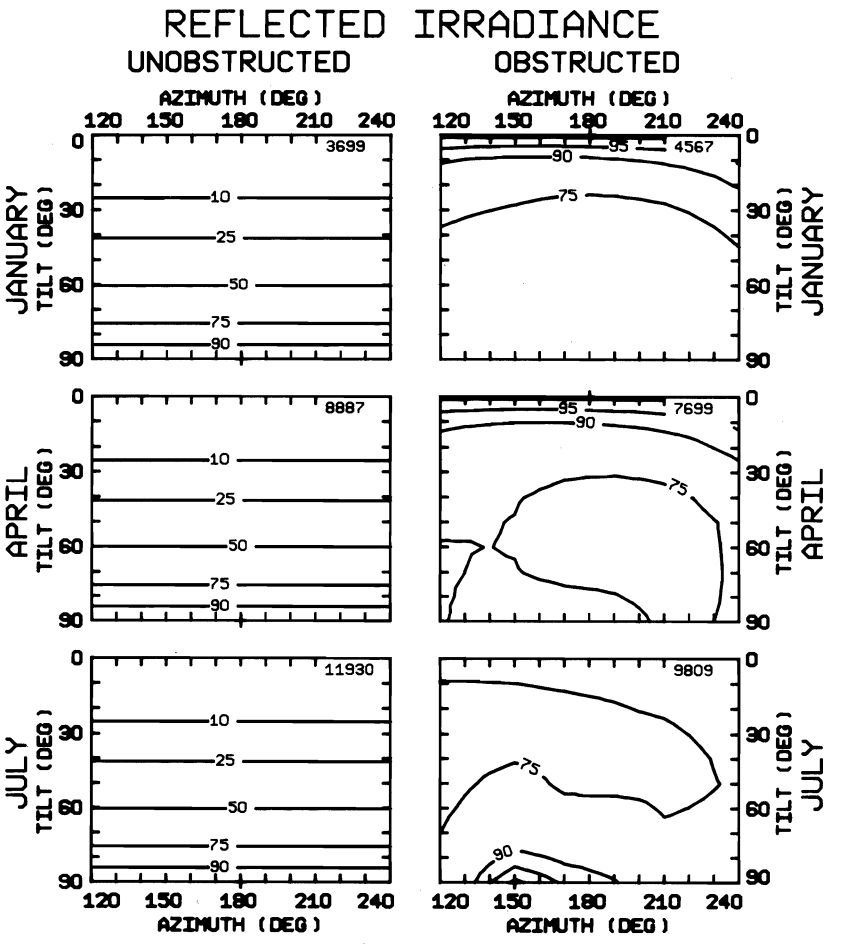

Fig. 6. Distribution of time-integrated reflected irradiance for each of the three simulated weeks. The '+' marks the collector orientation of maximal reflected irradiance receipt (given in the upper right-hand corner of each map (kJ m^{-2})) and the isolines are percentages of that maximum.

in total irradiance, therefore, can be attributed to the loss of isotropic diffuse radiation from sky and ground. Since direct beam irradiance is the largest component of total irradiance, no significant change in the optimal orientation of the collector—relative to that for an unobstructed site—was expected. However, because the maximal receipt of isotropic sky-diffuse irradiance is from the east and is almost half as large as direct-beam irradiance, the optimal azimuth of the obstructed collector in July shifts eastward 15°—to due south.

In order to estimate potential energy losses incurred by using popular engineering rules,† total irradiance for a collector 'sited' using each of three rules—tilt equal to the latitude, latitude +15° and latitude −15°—was interpolated from the output matrix of total irradiances for each simulation. The ratio of total irradiance at the rule-derived orientation to the simulated optimal total irradiance was subsequently determined for the six simulations (Table 1). For an unobstructed collector, the standard siting procedures work well. A collector whose tilt angle equals the latitude receives a large proportion of maximum total irradiance for all of the three seasons. Increasing the tilt angle by 15° results in a higher proportion of maximum total irradiance in January, while tilting the collector 15° less than the latitude gives the highest proportion of optimal in both April and July. In an obstructed environment, these rules of thumb do not work as

Table 1. Ratio of total irradiance on a collector sited using three rules of thumb to the total irradiance available on an optimally oriented collector as determined by simulation

Siting	Unobstructed			Obstructed		
Method	January	April	July	January	April	July
latitude + 15	0.999	0.919	0.753	0.863	0.880	0.723
latitude	0.977	0.936	0.833	0.923	0.963	0.872
latitude - 15	0.861	0.994	0.963	0.939	0.988	0.961

well because of the asymmetries in the irradiance distribution caused by the presence of the obstructions (Table 1). While the tilt of the optimally oriented collector showed little change due to the presence of horizonal obstructions, the optimal azimuth was as much as 60° away from due south. Application of the rule appropriate to each of the three obstructed scenarios resulted in 'losses' of almost 4% in both April and July while in January a reduction of almost 14% from the simulated optimal irradiance was found (Table 1).

In situations where there are no horizonal obstructions and no seasonal or diurnal asymmetries in global solar irradiance, general rules of thumb suggest orientations whose total irradiance is within 5% of the simulated optimum. However, in locations with marked asymmetries, simulations of collector irradiance predict optimal orientations that may receive as much as 15% more total irradiance than an appropriate rule of thumb-determined orientation.

5. SUMMARY AND CONCLUSIONS

A numerical climatic model has been developed in order to predict the irradiance on a fixed, flat-plate solar collector of any orientation. Measured global irradiance was, as a first step, partitioned into its direct-beam, isotropic-diffuse and anisotropic-diffuse components by the methods of Erbs [8] and Hay [16, 26]. Each component was then adjusted for non-horizontal orientations, shadowing and reflection. Irradiances were simulated for collector orientations that varied in 10° increments over a 120° range of azimuths centered on due south, and a range of tilts from horizontal to vertical. All the irradiance computations were made hourly for each collector orientation and then were integrated over three seasonally representative one week periods.

These simulations confirm, as expected, that the receipt of solar radiation by a collector can be substantially reduced by the presence of horizontal obstructions. In addition, it was found that the optimal collector azimuth may differ as much as 60° from due south when the horizon is obstructed. It also has been demonstrated that simple siting procedures may result in energy losses of as much as 10–15%—relative to the optimal orientation found by simulation—depending on climatic factors and the configuration of the horizonal obstructions.

Acknowledgement—Support from the Center for Climatic Research and the Computing Center at the University of Delaware is gratefully acknowledged. Any errors which have gone undetected, are entirely the responsibility of the authors.

NOMENCLATURE

$F(\Delta A_j \rightarrow dA_i)$ view factor between obstruction element and collector
G_j area of the view semicircle (on the ground) which is obstructed by obstruction j (m^2)
H_h global irradiance (kJ m^{-2})
H_{hb} direct-beam irradiance on a horizontal surface (kJ m^{-2})
H_{hd} total sky-diffuse irradiance on a horizontal surface (kJ m^{-2})
H_i total irradiance on a sloping, collector surface (kJ m^{-2})
H_{ib} direct-beam irradiance on a sloping, collector surface (kJ m^{-2})
H_{ida} anisotropic sky-diffuse irradiance on a sloping, collector surface (kJ m^{-2})
H_{idi} isotropic sky-diffuse irradiance on a sloping, collector surface (kJ m^{-2})
H_{idij} isotropic sky-diffuse irradiance on obstruction element j (kJ m^{-2})
H_{idr} diffuse irradiance on a sloping, collector surface that was reflected from the ground (kJ m^{-2})
H_{idrj} diffuse irradiance on collector element j that was reflected from the ground (kJ m^{-2})
H_{idro} diffuse irradiance on a sloping, collector surface that was reflected from horizonal obstructions (kJ m^{-2})
H'_i total irradiance on a sloping, collector surface after the correction for horizonal obstructions (kJ m^{-2})
H'_{ib} direct-beam irradiance on a sloping, collector surface after the correction for horizonal obstructions (kJ m^{-2})
H'_{ida} anisotropic sky-diffuse irradiance on a sloping, collector surface after the correction for horizonal obstructions (kJ m^{-2})
H'_{idi} isotropic sky-diffuse irradiance on a sloping, collector surface after the correction for horizonal obstructions (kJ m^{-2})
H'_{idr} diffuse irradiance on a sloping, collector surface that was reflected from the ground after the correction for horizonal obstructions (kJ m^{-2})
H'_{ij} total irradiance on obstruction element j after the correction for horizonal obstructions (kJ m^{-2})
H'_{ibj} direct-beam irradiance on obstruction element j after the correction for horizonal obstructions (kJ m^{-2})
H'_{idaj} anisotropic sky-diffuse irradiance on obstruction element j after the correction for horizonal obstructions (kJ m^{-2})
H_{nb} direct-beam irradiance at normal incidence (kJ m^{-2})
H_o instantaneous solar radiation on a horizontal surface at the outer atmosphere (kJ m^{-2})
H_{sc} solar constant (kJ m^{-2})
k_T hourly clearness index (H_h/H_o)
r radius of reflection from the ground onto the collector (m)
β tilt angle of a collector slope from horizontal (rad or deg)
κ_h anisotropy index for horizontal surfaces
κ_i anisotropy index for sloping surfaces
θ_i angle between a surface normal and the position vector of the sun (rad or deg)
θ_z zenith angle of the sun (rad or deg)
ρ albedo of the ground
ρ_j albedo of obstruction element j

REFERENCES

1. C. J. Willmott, On the climatic optimization of the tilt and azimuth of flat-plate solar collectors. *Solar Energy* **28**, 205–216 (1982).

2. C. M. Rowe, Simulation of shortwave irradiance on flat-plate solar collectors in urban environments. *Publs Clim* **35**(1), (1982).
3. G. Borgefors, *Optimal Positions of a Flat Solar-energy Collector for Selected Conditions and Geometries*. No. G320-3341, IBM Palo Alto Scientific Center, Palo Alto, California (1975).
4. W. H. Hoecker, *Relative Effective Solar Space Heating over the United States from Southward-tilted Solar Collectors*. NOAA Technical Memorandum ERL ARL-73, Air Resources Lab, Silver Spring, Maryland (1978).
5. J. Kern and I. Harris, On the optimal tilt of a solar collector. *Solar Energy* **17**, 97–102 (1975).
6. J. E. Hay, Calculation of monthly mean solar radiation for horizontal and inclined surfaces. *Solar Energy* **23**, 301–307 (1979).
7. B. Y. H. Liu and R. C. Jordan, The interrelationship and characteristic distribution of direct, diffuse and total solar radiation. *Solar Energy* **4**, 1–19 (1960).
8. D. G. Erbs, *Methods for Estimating the Diffuse Fraction of Hourly, Daily, and Monthly-average Global Solar Radiation*. Master thesis, University of Wisconsin-Madison (1980).
9. D. G. Erbs, S. A. Klein and J. A. Duffie, Estimation of the diffuse radiation fraction for hourly, daily and monthly-average global radiation. *Solar Energy* **28**, 293–302 (1982).
10. J. V. Dave, Validity of the isotropic-distribution approximation in solar energy estimations. *Solar Energy* **19**, 331–333 (1977).
11. K. Ya. Kondratyev, *Radiation regime of inclined surfaces*. Tech. Note No. 152, WMO-No. 467, World Meteorological Organization, Geneva (1977).
12. M. D. Steven, Standard distributions of clear sky radiance. *Q. Jl R. Met. Soc.* **103**, 457–465 (1977).
13. M. D. Steven and M. H. Unsworth, The diffuse irradiance of slopes under cloudless skies. *Q. Jl R. Met. Soc.* **105**, 593–602 (1979).
14. L. J. B. McArthur and J. E. Hay, An assessment of the techniques for determining the distribution of diffuse solar radiance for the sky hemisphere. *Solar Energy* **25**, 573–574 (1980).
15. L. J. B. McArthur and J. E. Hay, A technique for mapping the distribution of diffuse solar radiation over the sky hemisphere. *J. Appl. Meteorol.* **20**, 421–429 (1981).
16. J. E. Hay, Measurement and modelling of shortwave radiation on inclined surfaces, *Preprint Volume: Third Conference on Atmospheric Radiation*, pp. 150–153. American Meteorological Society, Boston, June (1978).
17. B. J. Garnier and A. Ohmura, A method of calculating the direct shortwave radiation income of slopes. *J. Appl. Meteorol.* **7**, 796–800 (1968).
18. B. J. Garnier and A. Ohmura, The evaluation of surface variations in solar radiation income. *Solar Energy* **13**, 21–34 (1970).
19. L. D. Williams, R. G. Barry and J. T. Andrews, Application of computed global radiation for areas of high relief. *J. Appl. Meteorol.* **11**, 526–533 (1972).
20. E. M. Sparrow and R. D. Cess, *Radiation Heat Transfer* (augmented ed.). Hemisphere, Washington (1978).
21. *Typical Meteorological Year User's Manual, TD-9734: Hourly Solar Radiation-Surface Meteorological Observations*. National Climate Center, Asheville, North Carolina (1981).
22. R. S. Frank, R. B. Gerding, P. A. O'Rourke and W. H. Terjung, Simulating urban obstructions. *Simulation* **36**, 83–92, March (1981).
23. A. J. Arnfield, An approach to the estimation of the surface radiative properties and radiation budgets of cities. *Phys. Geogr.* **3**, 97–122 (1982).
24. J. A. Duffie and W. A. Beckman, *Solar Engineering of Thermal Processes*. Wiley, New York (1980).
25. R. C. Temps and K. L. Coulson, Solar radiation incident upon slopes of different orientations. *Solar Energy* **19**, 179–184 (1977).
26. J. E. Hay, *Study of shortwave radiation on non-horizontal surfaces*. Report No. 79–12, Canadian Climate Centre, Atmospheric Environment Service, Downsview, Ontario (1979).
27. A. Eggers-Lura (Editor), *Flat plate solar collectors and their application to dwellings (low temperature conversion of solar energy)*. Study Contract No. 207-75-9 ECI DK, Commission of the European Communities, Copenhagen (1976).
28. K. W. Heinemann, *Thermal Applications of Solar Energy: a Professional Guide*. Garland STPM Press, New York (1981).
29. H. P. Garg, *Treatise on Solar Energy: Volume 1, Fundamentals of Solar Energy*. Wiley, Chichester (1982).
30. J. F. Kreider and F. Kreith, *Solar Heating and Cooling: Active and Passive Design* (2nd ed.). Hemisphere, Washington (1982).